

# Characteristic Study of the Boundary Layer Parameters over the Arabian Sea and the Bay of Bengal Using the QuikSCAT Dataset

V. HAMZA\*, C. A. BABU, and T. P. SABIN

*Department of Atmospheric Sciences, Cochin University of Science and Technology, Cochin-682 016, India*

(Received 10 January 2006; revised 16 January 2007)

## ABSTRACT

The marine atmospheric boundary layer (MABL) plays a vital role in the transport of momentum and heat from the surface of the ocean into the atmosphere. A detailed study on the MABL characteristics was carried out using high-resolution surface-wind data as measured by the QuikSCAT (Quick scatterometer) satellite. Spatial variations in the surface wind, frictional velocity, roughness parameter and drag coefficient for the different seasons were studied. The surface wind was strong during the southwest monsoon season due to the modulation induced by the Low Level Jetstream. The drag coefficient was larger during this season, due to the strong winds and was lower during the winter months. The spatial variations in the frictional velocity over the seas was small during the post-monsoon season ( $\sim 0.2 \text{ m s}^{-1}$ ). The maximum spatial variation in the frictional velocity was found over the south Arabian Sea ( $0.3$  to  $0.5 \text{ m s}^{-1}$ ) during the southwest monsoon period, followed by the pre-monsoon over the Bay of Bengal ( $0.1$  to  $0.25 \text{ m s}^{-1}$ ). The mean wind-stress curl during the winter was positive over the equatorial region, with a maximum value of  $1.5 \times 10^{-7} \text{ N m}^{-3}$ , but on either side of the equatorial belt, a negative wind-stress curl dominated. The area average of the frictional velocity and drag coefficient over the Arabian Sea and Bay of Bengal were also studied. The values of frictional velocity shows a variability that is similar to the intraseasonal oscillation (ISO) and this was confirmed via wavelet analysis. In the case of the drag coefficient, the prominent oscillations were ISO and quasi-biweekly mode (QBM). The interrelationship between the drag coefficient and the frictional velocity with wind speed in both the Arabian Sea and the Bay of Bengal was also studied.

**Key words:** boundary layer characteristics, drag coefficient, frictional velocity, roughness length, QuikSCAT wind

DOI: 10.1007/s00376-007-0631-7

---

## 1. Introduction

The marine atmospheric boundary layer (MABL) is the atmospheric layer located just above the sea surface and is influenced by the presence of that surface. It plays an important role in the exchange of momentum, mass and energy across the surface and also influences to a large extent the atmospheric and oceanic circulations. The wind patterns over the coastal areas, often show large differences over land in comparison to those over the sea. Many studies have been carried out to understand the atmospheric boundary layer characteristics over land. Since data collection over the sea via research cruises are expensive, the marine atmospheric boundary characteristics, especially

over the Arabian Sea and the Bay of Bengal, were studied in connection with a few field experiments. Some of the major experiments in this category are the Monsoon experiment-77 (MONEX-77), MONEX-79, Bay of Bengal monsoon experiment (BOBMEX-99) and Arabian Sea monsoon experiment (ARMEX). The Planetary Boundary Layer (PBL) process constitutes an important physical input into the numerical simulations of the monsoon (Rao, 1988; Krishnamurti et al., 1973; Manabe et al., 1974; Shukla et al., 1981) and PBL physics are usually incorporated into models by adopting suitable parameterization schemes (Kusuma et al., 1991).

Holt and Raman (1987) studied the structure of the boundary layer over the Arabian Sea and the Bay

---

\*Corresponding author: V. HAMZA, hamzavarikoden@yahoo.com

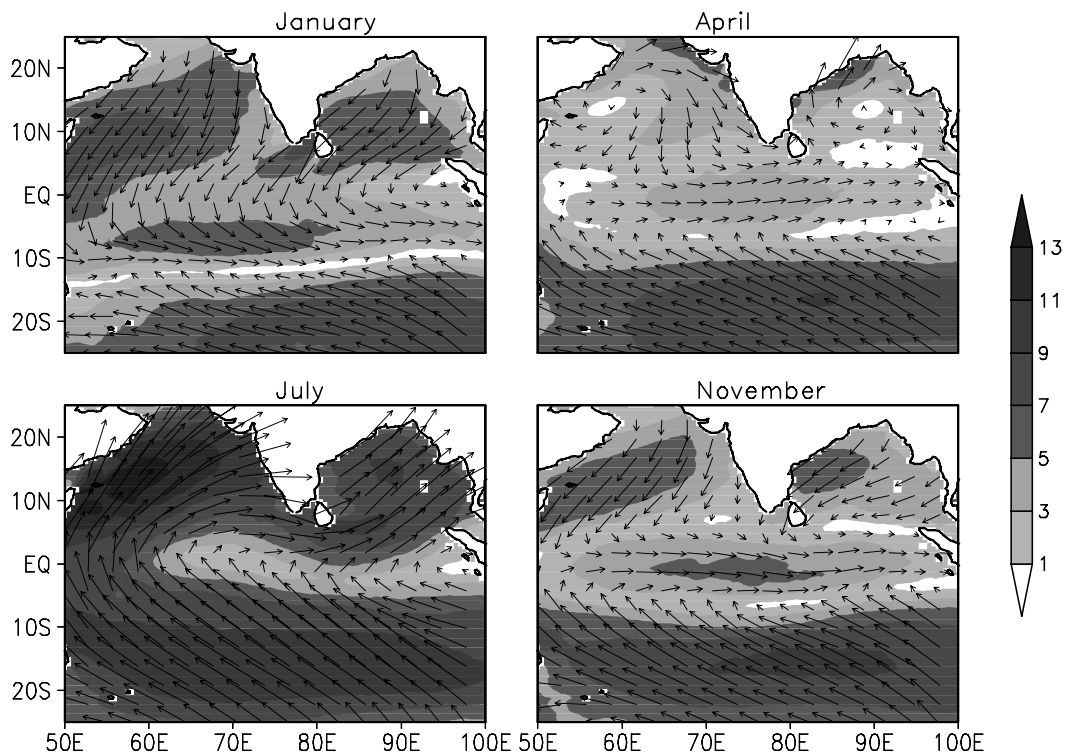


**Fig. 1.** Surface-wind speed ( $\text{m s}^{-1}$ ) distribution during the different seasons (composite for four years: 2000 to 2003).

of Bengal during both the active and break phases of the monsoon using the Indian-Soviet monsoon experiment (ISMEX-77) and the MONEX-79 dataset. They found that the height of the boundary layer decreased during the active phase and increased during weak phases of the monsoon. Sam et al. (2003) examined the temporal evolution of the turbulent kinetic energy, sensible and latent heat fluxes and the drag coefficient using radiosonde data taken from BOBMEX-99, during the different epochs of the Indian summer monsoon. They reported that the simulation results using a 1-D model agreed well with the observational analysis. TOGA COARE (Tropical Ocean Global Atmosphere Coupled Ocean Atmosphere Response Experiment), which was aimed to describe the coupling of the west Pacific warm pool to the atmosphere (Webster and Lukas, 1992), provided insight into the atmosphere-ocean coupling on an intraseasonal time scale (Godfrey and Lindstorm, 1989; Shinoda et al., 1998). The energy supplied by the atmosphere was mostly trapped in MABL, except in the regions of deep convection. So, it was very important to understand the various characteristics such as the drag coefficient, roughness length and other parameters of MABL. Mahrt and Ek (1993) studied the spatial variability of the turbulent fluxes and roughness lengths over a heterogeneous surface using flight

data collected during clear-sky days and found that the effective roughness length was about 1 m.

Here, we have made an attempt to explore the MABL characteristics over the Arabian Sea and the Bay of Bengal on a seasonal basis. The analysis was carried out on a seasonal basis by taking data from January for winter, April for pre-monsoon, July for the southwest monsoon and November for the post-monsoon seasons. The parameters employed for studying the characteristics of MABL were the drag coefficient, roughness length, frictional velocity and the wind-stress curl. To determine the variabilities on different time scales for the frictional velocity and drag coefficient, these parameters were subjected to wavelet analysis and the results are presented here.

## 2. Data and methods

The datasets used for this present study were the zonal and meridional components of the surface wind, wind stress and wind-stress curl for the period extending from 19 June 1999 to 30 December 2003 that were taken from the two-dimensional surface-wind fields that were measured by the SeaWinds scatterometer on the QuikSCAT satellite of the National Aeronautics and Space Agency (NASA) (Patoux and Brown, 2001; Wentz, 1986). In addition to the ERS-2 (Euro-

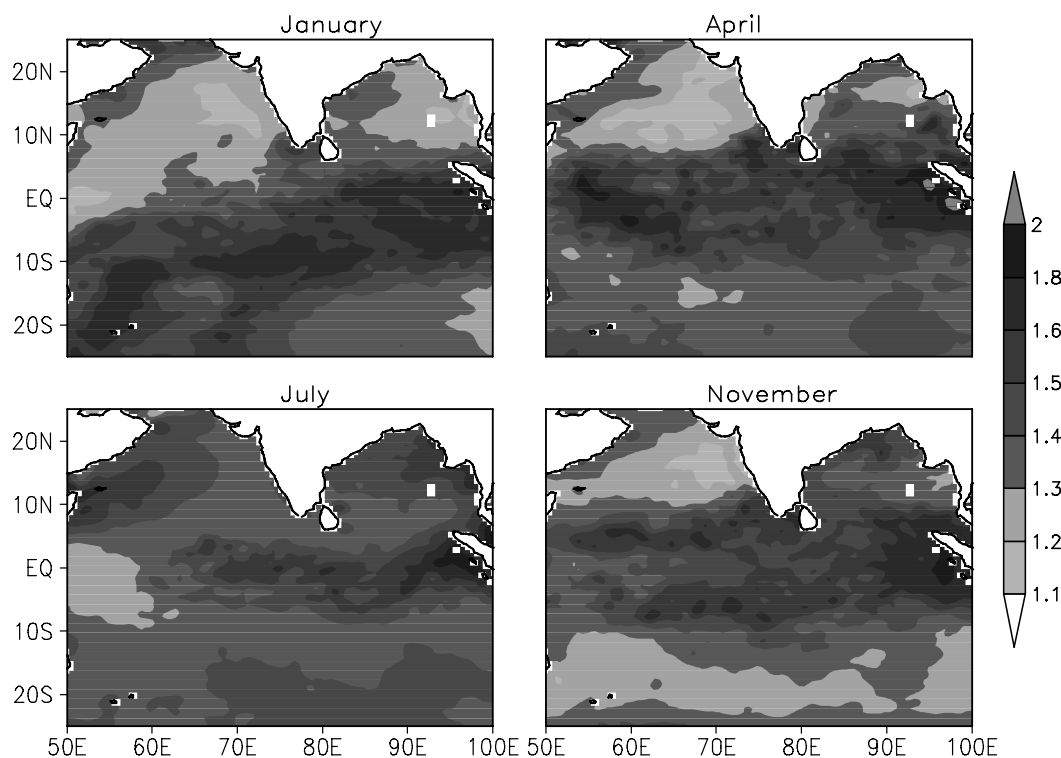


**Fig. 2.** Drag coefficient distribution derived from the QuikSCAT dataset during the different seasons, (composite for four years: 2000 to 2003).

pean Remotesensing Satellite) scatterometer that was launched by the European Space Agency (ESA) in April 1995, a new scatterometer, named SeaWinds, was launched onboard the QuikSCAT satellite by NASA/JPL (Jet Propulsion Laboratory) in June 1999. It was designed to observe wind vectors with an accuracy of 20 degrees in direction,  $2 \text{ m s}^{-1}$  in speed and a spatial resolution of 25 km. This high-resolution dataset can be used to derive a better understanding of the MABL and provides valuable information in regards to the atmospheric conditions over the oceans where it is very difficult to procure data from field experiments. Goswami and Rajagopal (2004) made comparisons between the QuikSCAT wind with *in situ* observations taken from various research cruises and found that this dataset agreed well with these observations. So, the surface information on wind vector and its products are reliable to estimate the drag coefficient, frictional velocity, roughness length and wind-stress curl on a seasonal basis.

To estimate the surface wind stress,  $\tau$ , for each scatterometer wind vector, the bulk formulation was used,

$$\tau = (\tau_x, \tau_y) = \rho C_d W(u, v),$$

where  $W$ ,  $u$ , and  $v$  are the scatterometer wind speed, zonal component (eastward) and meridional compo-

nent (northward), respectively. The surface wind was assumed to be parallel to the stress vector.  $\rho$  is the density of air and is equal to  $1.225 \text{ kg m}^{-3}$  and  $C_d$  is the drag coefficient. The magnitude of the stress is,

$$|\tau| = \rho C_d W.$$

There were many estimates of  $C_d$ . We selected the one published and recommended by Smith (1988), which was chosen by the WOCE community.

The frictional velocity  $u_*$  was obtained from the formula

$$u_* = \sqrt{\tau/\rho},$$

where  $\tau$  is the surface wind stress and  $\rho$  is the density of air. The roughness length,  $z_0$  is calculated using,

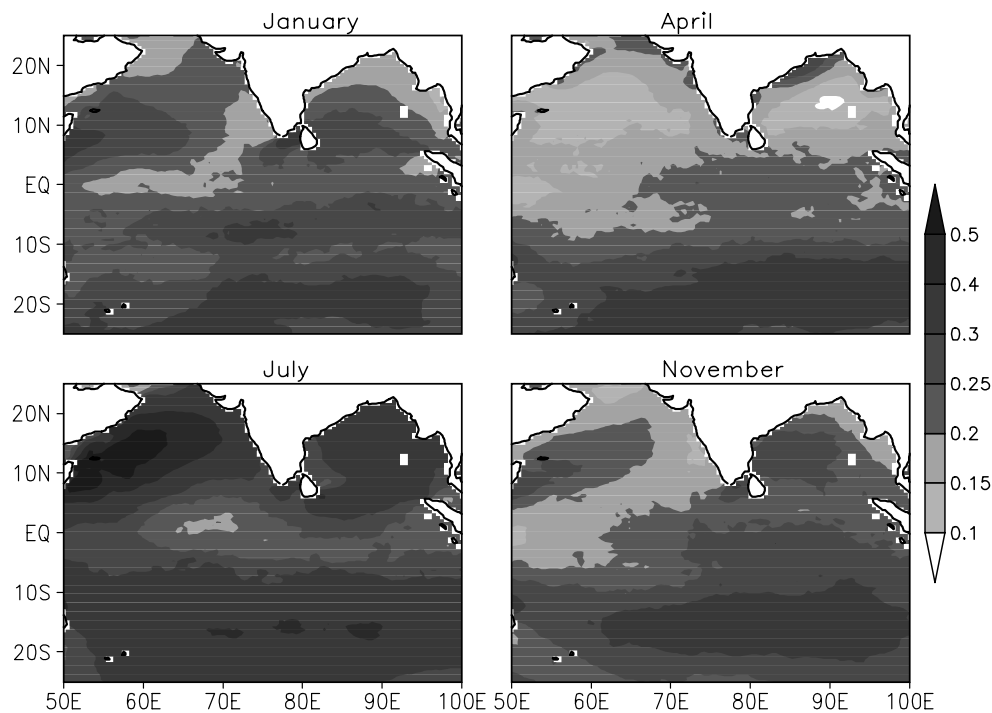
$$\bar{U} = \frac{u_*}{k} \ln \frac{z}{z_0},$$

where  $\bar{U}$  is the mean wind,  $k$  is von Kármán's constant with the value taken as 0.4 and  $z$  is the reference height (10 m).

### 3. Results and discussions

#### 3.1 Surface wind

The climatologies of the surface-wind patterns that were derived from the QuikSCAT SeaWinds scatterometer for the different seasons are presented in



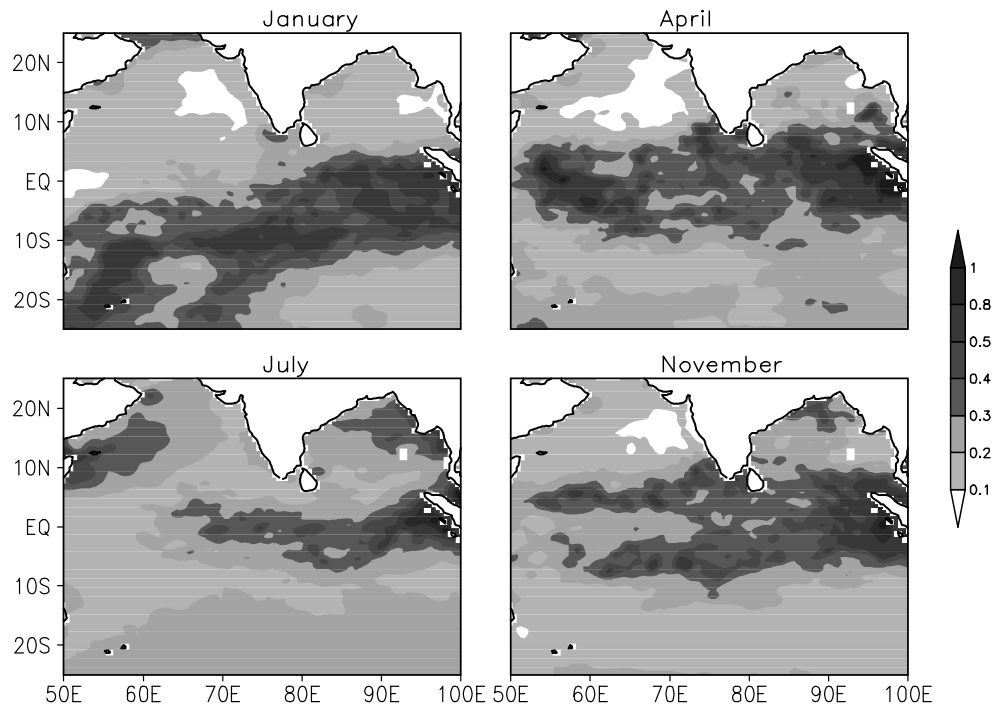
**Fig. 3.** Spatial variation in the frictional velocity ( $\text{m s}^{-1}$ ) for the different seasons, derived from the QuikSCAT dataset (composite for four years: 2000 to 2003).

Fig. 1. Here, the figures are presented over the region  $25^{\circ}\text{S}$ – $25^{\circ}\text{N}$  and  $50^{\circ}$ – $100^{\circ}\text{E}$  in order to bring out the features within the entire monsoon domain. In the figure, the left top panel shows the wind pattern for the winter (January), which represents northeasterly winds over the Arabian Sea and the Bay of Bengal, since January belongs to northeast monsoon season. In the south of  $10^{\circ}\text{S}$ , the prominent wind direction is southeasterly. The winds from the equatorial region and from  $20^{\circ}\text{S}$  converged around  $11^{\circ}\text{S}$  and blew towards the east. The top right panel of the figure shows similar features observed during the pre-monsoon season (April). During April, the surface winds were in a transitional stage from northeasterly to southwesterly and were weak both in the Arabian Sea and in the Bay of Bengal due to this transition. The winds over the west peninsular coastal belt was relatively stronger and the direction was northwesterly. In the Indian Ocean (south of the equator) the speed and direction of the winds were the same, but the convergence zone was shifted towards the north and occupied the area over the equator, however, the wind was weak in comparison to those prevalent during the winter. The wind patterns during the southwest monsoon (July) are presented in the left bottom panel of Fig. 1. Here, the surface wind was stronger in comparison to all other seasons measured and was due to the intensification of the surface winds by the Low Level Jetstream (LLJ).

The LLJ forms mainly over the Indian subcontinent during the southwest monsoon period with a wind core around 850 hPa (Joseph and Raman, 1966; Findlater, 1966). This strengthening of the surface winds results in the abundant transfer of moisture from the sea surface to the atmosphere over this region for the duration of the southwest monsoon. The bottom right panel of Fig. 1 presents the wind patterns during the post-monsoon season (November). During this period, the prominent surface-wind direction was northeasterly due to the influence of the post-monsoon and the strength was relatively low.

### 3.2 Drag coefficient

The drag coefficient ( $C_d$ ) is the bulk transfer coefficient of momentum.  $C_d$  has wide applications for the evaluation of the momentum flux and it has no unique value for either land or ocean surfaces. Many studies have been carried out in order to determine the values of  $C_d$  for both land and ocean positions. Garratt (1977) estimated the value of  $C_d$  over the Arabian Sea north of  $20^{\circ}\text{N}$  as  $3.9 \times 10^{-3}$  and over south of  $20^{\circ}\text{N}$  as  $27.7 \times 10^{-3}$ . Mohanty et al. (1996) estimated the value of over the western desert region and found it to be  $5.43 \times 10^{-3}$ , while Kusuma (1996) also presented values for Jodhpur and Kharagpur, using the MONTBLEX-90 dataset. Here,  $C_d$  was computed using the equation as described in the methodology. Figure 2 shows the



**Fig. 4.** Spatial variation of roughness length (mm) in different seasons derived from the QuikSCAT dataset (composite of four years: 2000 to 2003).

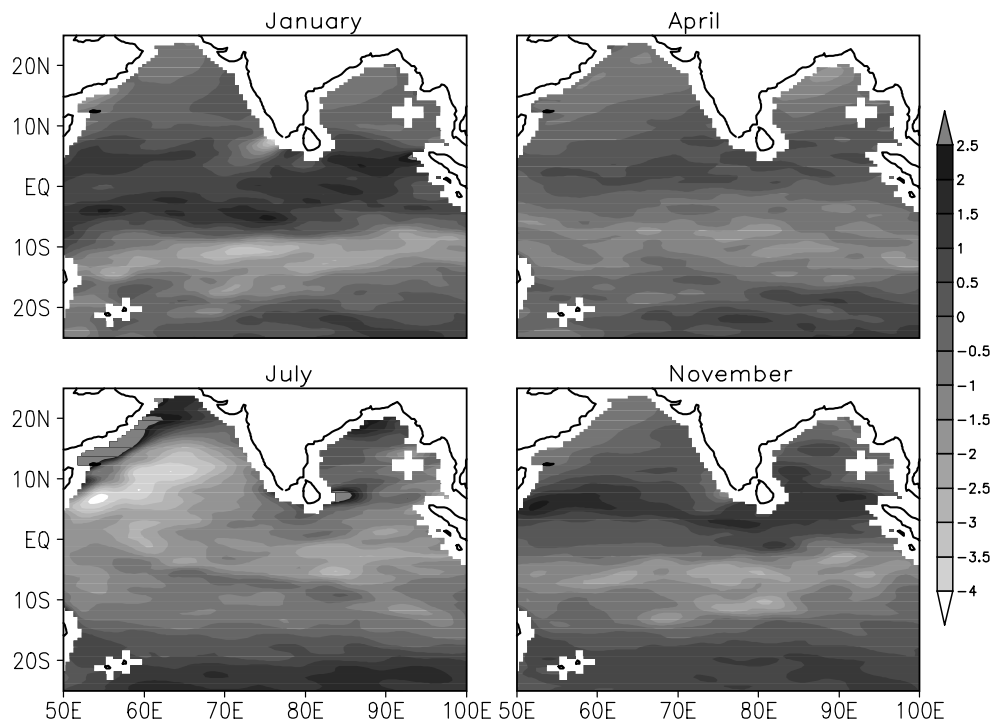


**Fig. 5.** Spatial variation in the wind-stress curl ( $N\ m^{-3}$ ) for the different seasons (composite for four years: 2000 to 2003).

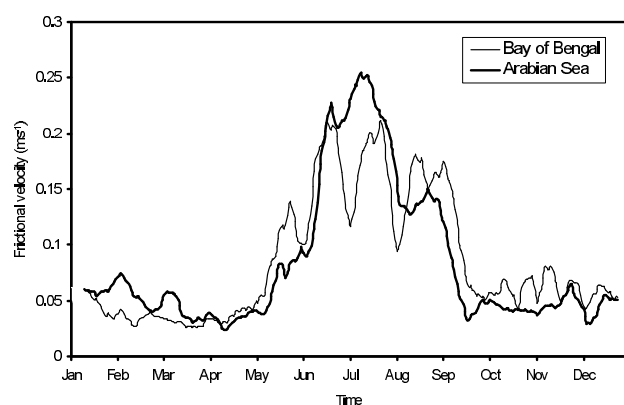


**Fig. 6.** 10-day moving average of the frictional velocity over the Arabian Sea (solid line,  $15^{\circ}$ – $20^{\circ}$ N,  $65^{\circ}$ – $70^{\circ}$ E) and the Bay of Bengal (light line,  $15^{\circ}$ – $20^{\circ}$ N,  $87^{\circ}$ – $92^{\circ}$ E).

mean  $C_d$  values for the winter (top left), pre-monsoon (top right), southwest monsoon (bottom left) and post-monsoon (bottom right). During the winter, the value was comparatively low in the area over the central Arabian Sea, with a value around  $1.2 \times 10^{-3}$ . In most of the areas of the Bay of Bengal, the value for was around  $1.35 \times 10^{-3}$ . During the pre-monsoon season, the values were less ( $1.2 \times 10^{-3}$ ) over the Arabian Sea and larger ( $1.35 \times 10^{-3}$ ) over the Bay of Bengal. The value over the central portion of the Arabian Sea was around  $1.2 \times 10^{-3}$  and it was more than  $1.4 \times 10^{-3}$  over the Bay of Bengal. During the southwest monsoon season, the  $C_d$  value was high over the Arabian Sea ( $1.5 \times 10^{-3}$ ), but was rather low ( $1.45 \times 10^{-3}$ ) over the Bay of Bengal. This may be due to the prevailing high wind speeds observed during the southwest monsoon season. During the post-monsoon season, the  $C_d$  values were larger ( $1.9 \times 10^{-3}$ ) over the Bay of Bengal than they were over the Arabian Sea. Among the four seasons, the maximum value of  $C_d$  was found during the post-monsoon season over the Bay of Bengal. These values were almost comparable, but slightly less than those reported by Garratt (1977) for the Arabian Sea. In general, the  $C_d$  values were less over the central Bay of Bengal and increased towards the coast. This may be due to the frictional effect of the land surface.

### 3.3 Frictional velocity

Frictional velocity is the scaling parameter of wind speed (Stull, 1997). It can be evaluated from the surface wind stress data available within the QuikSCAT dataset. Figure 3 provides the frictional velocity ( $u_*$ ) over the Arabian Sea and the Bay of Bengal during all four seasons. During the winter, the spatial variations in  $u_*$  were small, both in the Arabian Sea and

in the Bay of Bengal. Satyanarayana et al. (2001) found that the frictional velocity during February and March varied between  $0.1 \text{ m s}^{-1}$  and  $0.25 \text{ m s}^{-1}$  in the south Arabian Sea and the values were slightly larger in the equatorial region of the Bay of Bengal. The results presented here are also comparable with those results. The contours of  $u_*$  are oriented with values increasing towards the north and with slightly higher values in the Bay of Bengal. During the pre-monsoon season, the value of  $u_*$  over the Arabian Sea was around  $0.15 \text{ m s}^{-1}$  and over the Bay of Bengal it was between 0.1 and 0.25, centered near the central Bay of Bengal region and was surrounded by contours of increasing values. The  $u_*$  values were higher during the southwest monsoon season in comparison to other seasons. The highest values (greater than  $0.55 \text{ m s}^{-1}$ ) were found near the Somali coast in the Arabian Sea. In the Bay of Bengal, the highest value was more than  $0.38 \text{ m s}^{-1}$  over the central Bay and was surrounded by lower values. The horizontal variations in the frictional velocity over both the Arabian Sea and the Bay of Bengal were small during the post-monsoon season with the value falling around  $0.2 \text{ m s}^{-1}$ . The maximum spatial variation in the frictional velocity among the four seasons occurred during the southwest season over the south Arabian Sea, varying from  $0.3 \text{ m s}^{-1}$  to  $0.5 \text{ m s}^{-1}$ , followed by the variations during the pre-monsoon season over the Bay of Bengal, which varied from  $0.1 \text{ m s}^{-1}$  to  $0.25 \text{ m s}^{-1}$ .

### 3.4 Roughness length

The roughness length ( $z_0$ ) is the distance from the surface to the point where the wind velocity transitions from zero to a non-zero value. Generally, information on  $z_0$  is derived using data observed in connection with field experiments over either land or ocean. Since it is difficult to take such observations during all seasons, over entire region, the characteristic features of  $z_0$  have not been properly studied. However, through the advent of high-resolution satellite-derived wind data, this parameter can be evaluated reliably. The spatial distribution of  $z_0$  is presented in the Fig. 4 for the winter, pre-monsoon, southwest monsoon and post-monsoon seasons. During the winter,  $z_0$  values varied from 0.2 mm to 1 mm and were larger than 0.5 mm over the entire coastal belt, with the exception of over the Sri Lankan region. The values were higher (more than 1 mm) over the north Arabian Sea and Somali coast. During the pre-monsoon season,  $z_0$  was more than 9 mm over the entire south Bay of Bengal and the coastal regions of Somali due to the feeble winds observed over these regions during the transitional period. During the southwest monsoon season, the values were extremely low (in the range of  $10^{-4}$

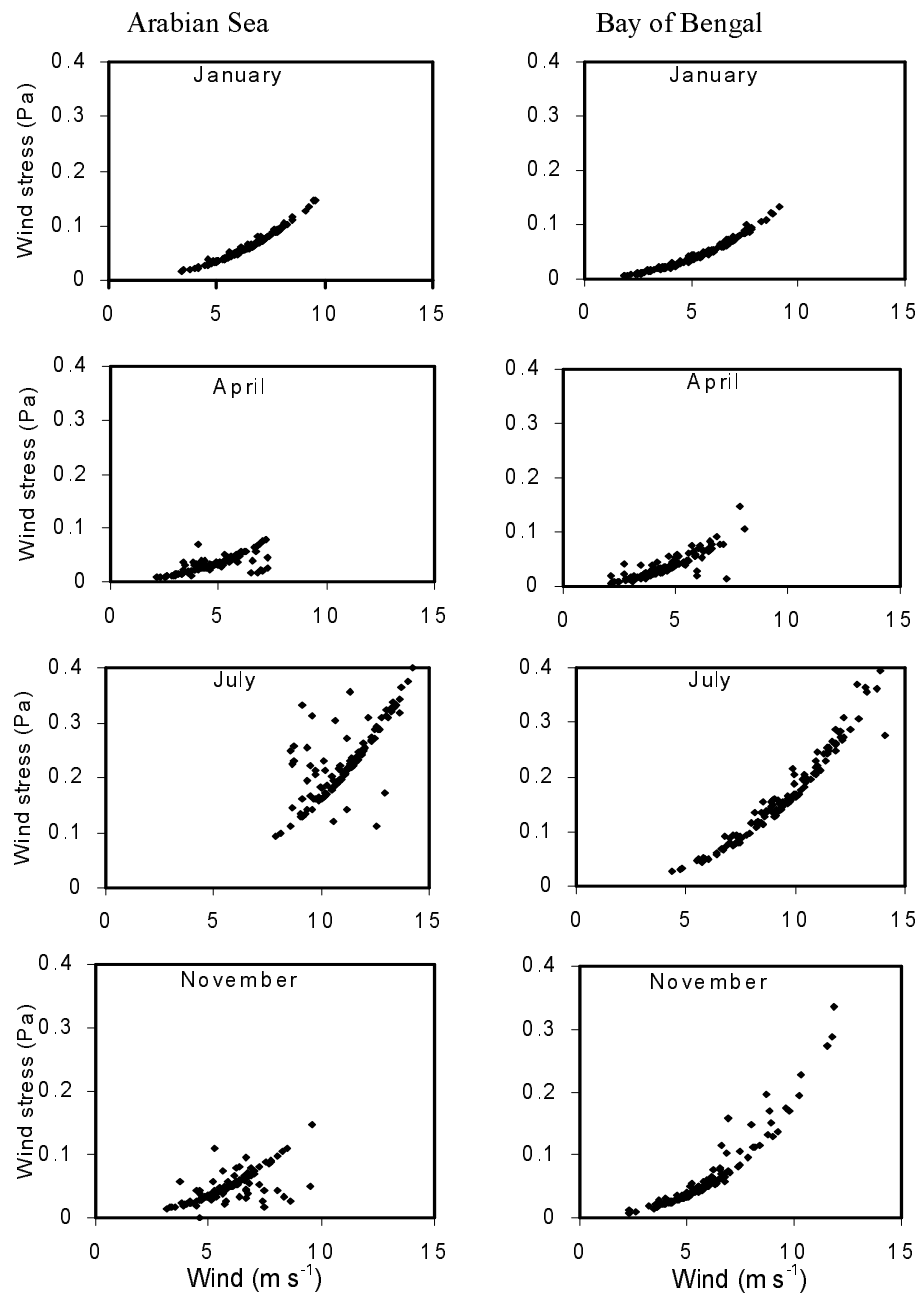


**Fig. 7.** The relationship between the surface wind stress and the wind speed during the different seasons over both the Arabian Sea and the Bay of Bengal.

mm), both over the Arabian Sea and the Bay of Bengal due to the high wind speeds associated with the monsoon. In the post-monsoon season, there were regions with small values for the parameter ( $< 1 \times 10^{-4}$ ) over the southwest Arabian Sea and central Bay of Bengal. High  $z_0$  values were found over the west peninsular region (more than 1 mm), over the head Bay of Bengal (more than 9 mm) and south of the Bay of Bengal (more than 10 mm). The range for  $z_0$  was at a maximum in both the Arabian Sea and the Bay of

Bengal during the post-monsoon season, due to the large spatial variations in the wind.

### 3.5 Wind-stress curl

The wind-stress curl depends mainly on the surface wind. It is a measure of the rotation of the force that is applied by the wind. The zonal wind stress in the equatorial region was westerly during pre-monsoon season and largest during both the spring and fall, thereby driving the equatorial spring and fall jets into

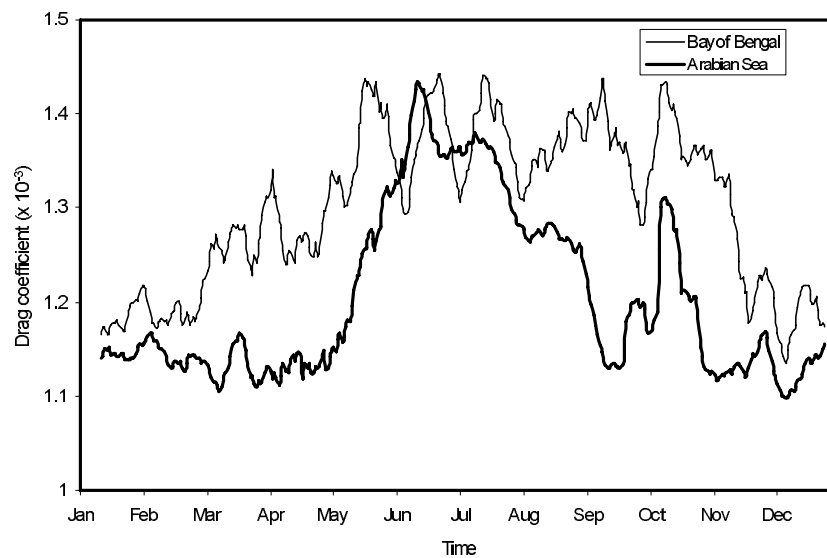


**Fig. 8.** 10-day moving average of the drag coefficient over the Arabian Sea (solid line,  $15^{\circ}$ – $20^{\circ}$ N,  $65^{\circ}$ E– $70^{\circ}$ E) and the Bay of Bengal (light line,  $15^{\circ}$ – $20^{\circ}$ N,  $87^{\circ}$ – $92^{\circ}$ E).

the Indian Ocean (Wyrski, 1973). The atlas by Hasenrath and Lamb (1979) gave a complete reference to the atmospheric fields over the equatorial region. The climatological surface wind stress and curl of the wind stress showed a maximum amplitude in the region off the coast of Somalia (Hellerman and Rosenstein, 1983). However, the curl changes its sign during northeast and southwest monsoon seasons. Here, we made an attempt to study the wind-stress curl over the different parts of the Arabian Sea and Bay of Bengal during the four seasons and also influence of the monsoon activity on the wind-stress curl. The mean distribution of the wind-stress curl is presented in Fig. 5. The winter season was characterized by a cyclonic stress (positive values) over the equatorial region ( $10^{\circ}$ N to  $10^{\circ}$ S) with a maximum value of  $1.5 \times 10^{-7} \text{ N m}^{-3}$ , but on either side of the equatorial belt, an anti-cyclonic stress was observed. The maximum value was found to be approximately  $-1.5 \times 10^{-7} \text{ N m}^{-3}$ , but on the northern side, the value of the negative stress was smaller ( $-0.5 \times 10^{-7} \text{ N m}^{-3}$ ). During the pre-monsoon period, the area and intensity of the cyclonic stress was decreased. Over the southern portion, the anti-cyclonic stress increased and shifted towards the north. During the southwest monsoon season, the cyclonic stress was extended into both the Arabian Sea and Bay of Bengal, with the value (larger than  $-3.5 \times 10^{-7} \text{ N m}^{-3}$ ) of the stress curl being larger over the east-central Arabian Sea (near the Somali coast). But near Sri Lanka, the anti-cyclonic wind-stress curl was noticed. During the post-monsoon season, positive values were found over the equatorial re-

gion and negative values were seen on either side of the equatorial belt.

### 3.6 Frictional velocity and drag coefficient over Arabian Sea and Bay of Bengal

#### 3.6.1 Frictional velocity

To examine the features of the frictional velocity over the Arabian Sea and Bay of Bengal, we found the area-weighted average of the velocity scale ( $u_*$ ) computed over the regions between  $15^{\circ}$ – $20^{\circ}$ N and  $65^{\circ}$ – $70^{\circ}$ E (Arabian Sea) and  $15^{\circ}$ – $20^{\circ}$ N and  $87^{\circ}$ – $92^{\circ}$ E (Bay of Bengal) for the period from 1 January 2000 to 31 December 2003. The 10-day moving-average values of the composite of the 4 years (2000 to 2003) is represented in Fig. 6, in which the solid line indicates the values for the Arabian Sea and dotted line indicates those for the Bay of Bengal. It was observed that the values for  $u_*$  in both the Arabian Sea and Bay of Bengal were found to be around  $0.05 \text{ m s}^{-1}$  from January until the first week in May. After the first week of May, the values over both the Arabian Sea and the Bay of Bengal increased, reaching to about  $0.2 \text{ m s}^{-1}$  by the end of May. During the monsoon season, the value were different in the two regions. In the Arabian Sea the value increased from the first week of May until the end of July (the value reached a maximum of  $0.25 \text{ m s}^{-1}$ ) and then decreased almost constantly until the end of September. The increase in within this region was attributed to the monsoon surge that was associated with LLJ and the consequential amplification of the surface wind. In the Bay of Bengal, the values of  $u_*$  were almost the same as those in the Arabian Sea,

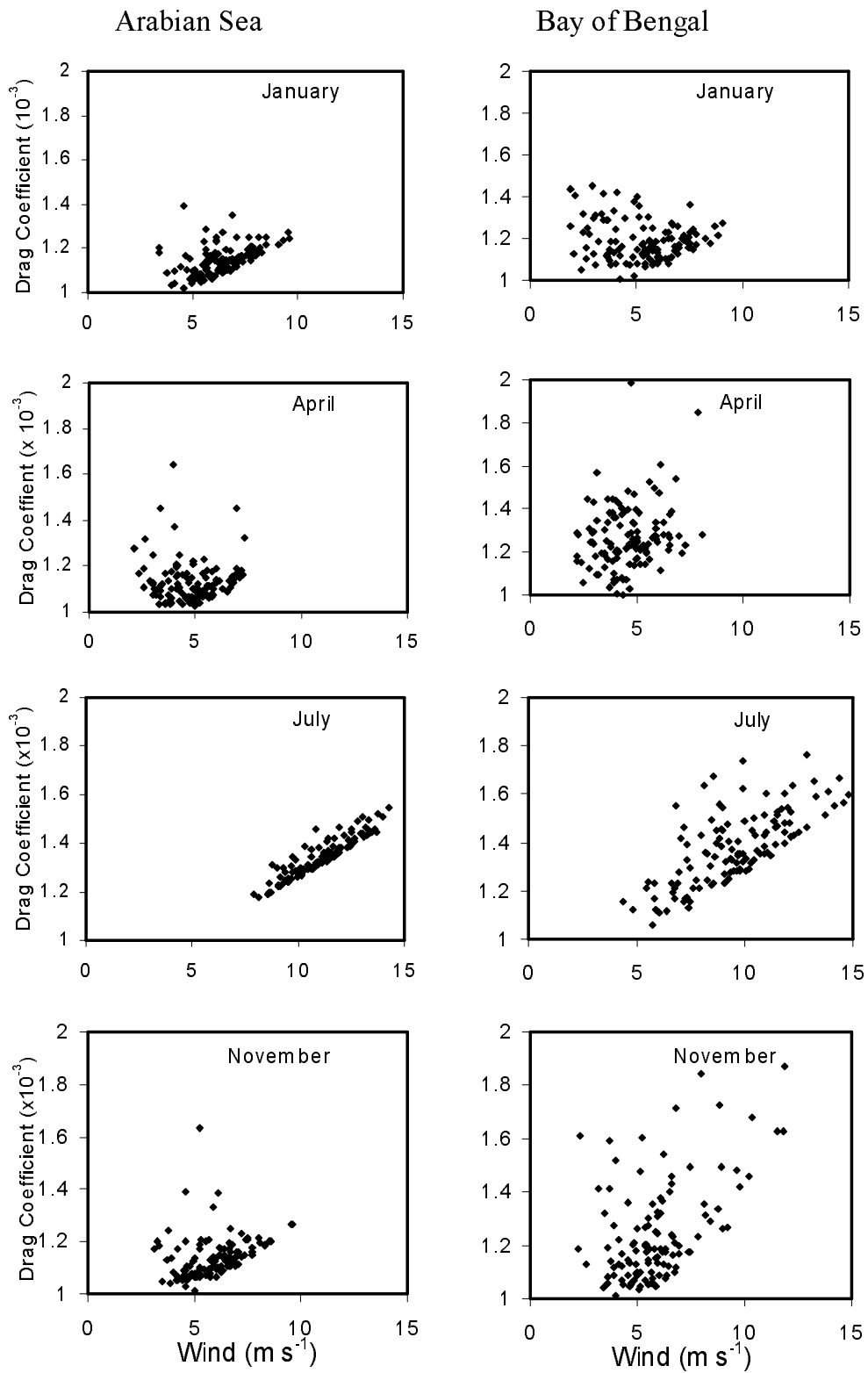


**Fig. 9.** Relationship between the drag coefficient and the wind speed during the different seasons over both the Arabian Sea and the Bay of Bengal.

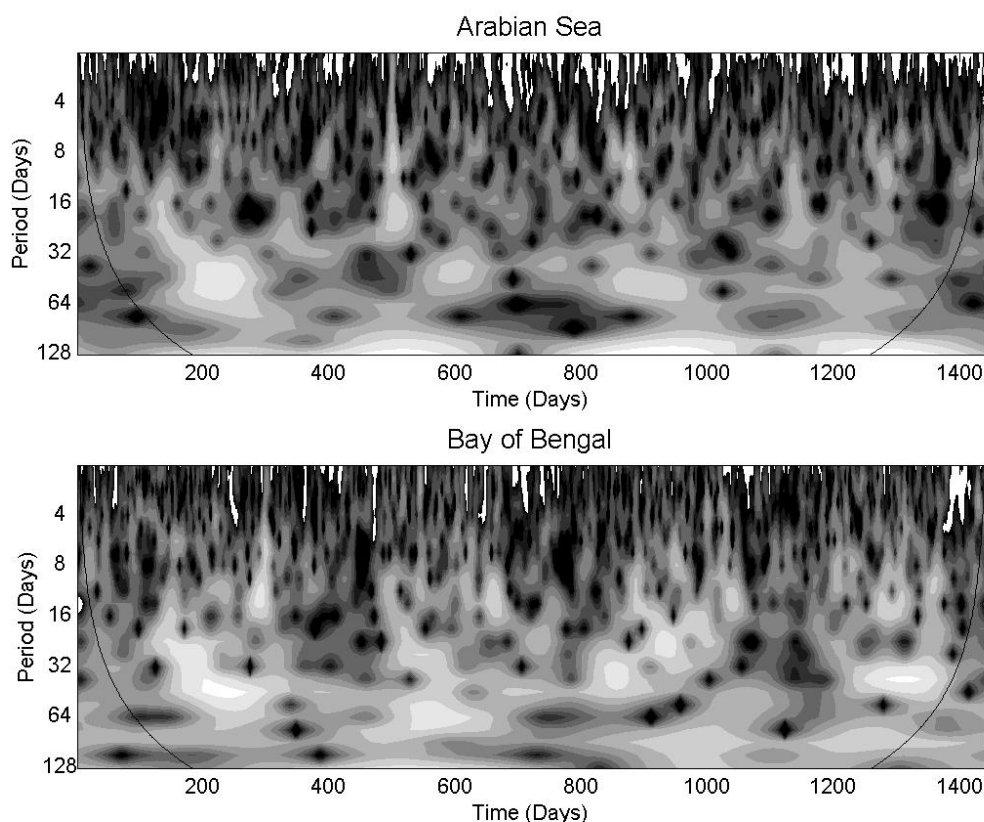


**Fig. 10.** Wavelet analysis of the frictional velocity over both the Arabian Sea and the Bay of Bengal.

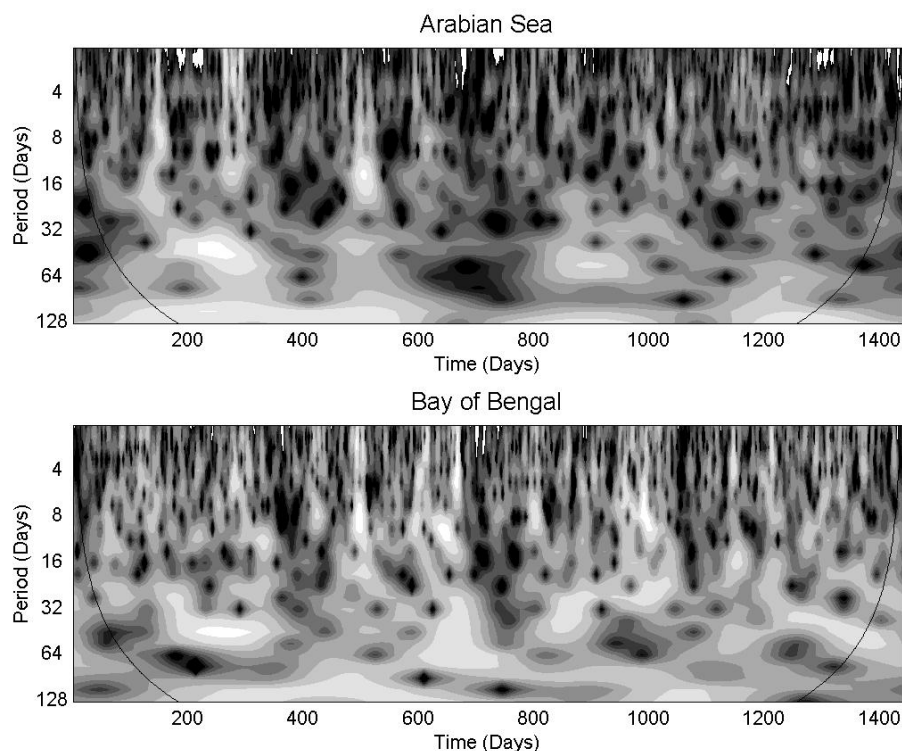
with the exception of during the monsoon season. During this period, the  $u_*$  increased and reached a maximum by the middle of June and then decreased. This pattern for  $u_*$  was maintained until the end of the monsoon period. The variability of  $u_*$  in the Bay of Bengal was attributed to the active and break cycles in the Indian summer monsoon. These monsoon epochs, especially the wind pattern, were more prominent in the Bay of Bengal than they were in the Arabian Sea. As the monsoon receded, the values returned to normal. This situation is the same over the Arabian Sea and the Bay of Bengal.

Figure 7 shows the inter-relationship between the wind speed and the wind stress over the Arabian Sea and the Bay of Bengal for the different seasons. In all of the seasons, the wind stress had a similar relationship to the wind field. Since wind stress depends on the square of the wind speed, it is a non-linear relationship. Viz, the stress versus wind speed trace curves upward with increasing wind speed. For lower wind speed, the wind stress was lower. Over the Arabian Sea, as the wind speed increased, the wind stress increased rapidly, resulting in a power-law fit. On the basis of the inter-relationship, one can obtain an equa-

tion to evaluate the wind stress as a function of the wind speed at any location in either the Arabian Sea or the Bay of Bengal during any season.

### 3.6.2 Drag coefficient

The features of  $C_d$  over the areas above the Arabian Sea and the Bay of Bengal are depicted in Fig. 8. It was found that the values for  $C_d$  in both the Arabian Sea and the Bay of Bengal are different, with the higher values being found over the Bay of Bengal during the entire period studied. In general, the pattern varied with season. Over the Arabian Sea, the values were almost constant ( $1.14 \times 10^{-3}$ ) during the period from November to May. During the monsoon period,  $C_d$  values were higher. From first week of May, the values increased, reaching a maximum by the first week of June ( $1.42 \times 10^{-3}$ ) and then slowly decreasing. In the Bay of Bengal,  $C_d$  values increased from the first week of March and reached a maximum during the monsoon season ( $1.35 \times 10^{-3}$ ). The variability of  $C_d$  in the Bay of Bengal was larger than that observed over the Arabian Sea, especially during the monsoon season.  $C_d$  values were found to decrease after the withdrawal of the monsoon, by the middle of November.



**Fig. 11.** Wavelet analysis of the drag coefficient over both the Arabian Sea and the Bay of Bengal.

The variations in  $C_d$  were also drawn for different years for both the Arabian Sea and the Bay of Bengal. Figure 9 represents the interrelationship between  $C_d$  and wind speed over the Arabian Sea and the Bay of Bengal, respectively. The Bay of Bengal showed a similar trend as that which was observed for the Arabian Sea. The variations in the drag coefficient with wind speed were not linear, but instead, the drag coefficient increased when the wind speed either increased or decreased from a critical value of  $4 \text{ m s}^{-1}$ .

### 3.7 *Intraseasonal variations in frictional velocity and drag coefficient*

The intraseasonal oscillation (ISO) is one of the major oscillations that is observed in the parameters of the lower atmosphere over the equatorial region that is associated with the northward/north-eastward propagation of the monsoon surge during the season (Yasunari, 1979, 1981; Sikka and Gadgil, 1980; Krishnamurti and Subramaniam, 1982). This ISO has two major components, which are either a 30–60 day and 10–20 day mode, which can be seen in the spectral analysis of the precipitation, convection and in many circulation parameters (Chen and Chen, 1993; Numaguti, 1995; Kiladis and Wheeler, 1995). Using the wavelet technique suggested by Torrence and Compo

(1998), we unraveled the different time-frequency domains that are embedded in the MABL parameters, such as the frictional velocity and drag coefficient. Figure 10 represents the wavelet analysis of the frictional velocity in the Arabian Sea and the Bay of Bengal. Daily values of the frictional velocity were taken from 1 January 2000 to 31 December 2003 and have been used for this analysis. From the figure, it is evident that the variability in the frictional velocity was different in the Arabian Sea and the Bay of Bengal. In the Arabian Sea, the variability around 60 day was prominent, with a 95% confidence level and this variability exhibited a periodicity of 35–64 days. But in the Bay of Bengal, this variability was found to be larger and varied from 25 day to 65 day, with the variability around 60 day having a confidence of 95% during the southwest-monsoon season. The confidence level varied from year to year. The variability under the 10–20 day mode also exists, but this variation was found during all seasons with a 99% confidence. Figure 11 presents the wavelet analysis for the drag coefficient. It was found that the variability of the drag coefficient was different for the Arabian Sea and the Bay of Bengal, similar to what was observed for the frictional velocity. In the Bay of Bengal, the variability with a 40–55 day mode was seen in all years during the monsoon months, with a

95% confidence level. But in the Arabian Sea, it was evident only during the monsoon months for the years 2000 and 2002. The 10–20 day mode (QBM) was also significant in the Bay of Bengal during all seasons.

#### 4. Conclusions

The average surface wind from 2000 to 2003 (4 years) during January, April, July, and November over the monsoon domain were examined and the results are highlighted herein. The values of  $C_d$  and  $u_*$  were larger during the southwest monsoon season in comparison to the other seasons. This is due to the increase in the surface-wind speed that is associated with the southwest monsoon low-level jetstream. The maximum spatial variation in the frictional velocity also occurred during this season over the south Arabian Sea, with the values ranging from  $0.3 \text{ m s}^{-1}$  to  $0.5 \text{ m s}^{-1}$ , followed by the pre-monsoon season over the Bay of Bengal, which saw values varying from  $0.1 \text{ m s}^{-1}$  to  $0.25 \text{ m s}^{-1}$ . The wind-stress curl during the winter season was positive over the equatorial region, with negative values being observed to either side of the equatorial belt. The area-average value of  $u_*$  in both the Arabian Sea and Bay of Bengal was found to be around  $0.05 \text{ m s}^{-1}$  from January until the first week of May, due to the lower wind strength. In the Arabian Sea, the value increased from first week of May until the end of July and then decreased consistently until the end of September. In the Bay of Bengal, an oscillation in was observed during the southwest-monsoon period, followed by a recession after the monsoon back to the original value. The surface-wind pattern and its variability over the Arabian Sea and the Bay of Bengal were different during the southwest season. The interrelationship between and the wind speed was prominent during January, but in all other seasons they showed scattered values from the trend line for both the Arabian Sea and the Bay of Bengal. In the case of the drag coefficient, the variability was more prominent during the southwest monsoon season and more obvious in the Arabian Sea than in the Bay of Bengal. The frictional velocities and drag coefficients over the Arabian Sea and the Bay of Bengal during the southwest-monsoon season, showed significant intraseasonal variability. The variabilities in the Arabian Sea and the Bay of Bengal were different however. The major oscillation in the Arabian Sea was intraseasonal oscillation, but in the Bay of Bengal, intraseasonal oscillation as well as quasi-biweekly mode was significant.

**Acknowledgements.** The authors are thankful to the ISRO-RESPOND, India for providing the financial sup-

port to this work.

#### REFERENCES

- Chen, T.-C., and J.-M. Chen, 1993: The 10–20 day mode of the 1979 Indian monsoon: Its relation with time variation of monsoon rainfall. *Mon. Wea. Rev.*, **121**, 2465–2482.
- Findlater, J., 1966: Cross equatorial jet streams at low levels over Kenya. *Meteor. Mag.*, **95**, 353–364.
- Garratt, J. R., 1977: review of the drag coefficients over the oceans and continents. *Mon. Wea. Rev.*, **105**, 915–929.
- Godfrey, J. S., and E. J. Lindstorm, 1989: On the heat budget of the equatorial west pacific surface mixed layer. *J. Geophys. Res.*, **94**, 8007–8017.
- Goswami, B. N., and E. N. Rajagopal, 2004: Indian Ocean surface winds from NCMRWF analysis as compared to QuikSCAT and moored buoy winds. *Proceedings of Indian Academy of Sciences (Earth and Planetary Sciences)*, **112**, 61–77.
- Hastenrath, S., and P. J. Lamb, 1979: *Climatic Atlas of the Indian Ocean*. Part I: Surface climate and atmospheric circulation. University of Wisconsin Press, Madison, USA, 247pp.
- Hellerman, S., and M. Rosenstein, 1983: Normal monthly mean wind stress over the world ocean with error estimates. *J. Phys. Oceanogr.*, **4**, 145–167.
- Holt, T., and S. Raman, 1987: The study of mean boundary layer structures over the Arabian Sea and the Bay of Bengal during active and break monsoon periods. *Bound.-Layer Meteor.*, **38**, 73–94.
- Joseph, P. V., and P. L. Raman, 1966: Existence of low level westerly jetstream over peninsular India during July. *Indian Journal of Meteorology and Geophysics*, **17**, 407–410.
- Kiladis, G. N., and M. Wheeler, 1995: Horizontal and vertical structure of observed tropospheric equatorial Rossby waves. *J. Geophys. Res.*, **100**(D), 22981–22997.
- Krishnamurti, T. N., and D. Subramaniam, 1982: The 30–50 day mode at 850 mb during MONEX. *J. Atmos. Sci.*, **39**, 2088–2095.
- Krishnamurti, T. N., M. Kanamitsu, B. Cesulski, and M. B. Mathui, 1973: Florida state university tropical prediction model. *Tellus*, **6**, 523–535.
- Kusuma, G. R., 1996: Roughness length and drag coefficient at two MONTBLEX–90 tower stations. *Proceedings of Indian Academy of Sciences (Earth and Planetary Sciences)*, **105**, 273–287.
- Kusuma, G. R., S. Raman, and A. Prabhu, 1991: Boundary layer heights over the monsoon trough region during active and break phases. *Bound.-Layer Meteor.*, **57**, 129–138.
- Mahrt, L., and M. Ek, 1993: Spatial variability of turbulent fluxes and roughness lengths in Hapex-mobilhy. *Bound.-Layer Meteor.*, **65**, 381–400.
- Manabe, S., D. G. Hahn, and J. Holloway, 1974: The seasonal variation of the tropical circulation as esti-

- mated by a global model of the atmosphere. *J. Atmos. Sci.*, **32**, 48–83.
- Mohanty, U. C., P. S. Parihar, and T. Venugopal, 1996: Estimation of drag coefficient over the western desert sector of the Indian summer monsoon trough. *Proceedings of Indian Academy of Sciences (Earth and Planetary Sciences)*, **104**, 273–287.
- Numaguti, A., 1995: Characteristics of 4- to 20-day period disturbances observed in the equatorial Pacific during the TOGA COARE IOP. *J. Meteor. Soc. Japan*, **73**, 353–377.
- Patoux, J., and R. A. Brown, 2001: A scheme for improving scatterometer surface wind fields. *J. Geophys. Res.*, **106**, 23995–24005.
- Rao, K. G., 1988: Diagnosis of dominant forcing factors for large scale vertical velocities during active and break phases of monsoon. *Pure and Applied Geophysics*, **127**, 669–693.
- Sam, N. V., U. C. Mohanty, and A. N. V. Satyanarayan, 2003: Simulation of marine boundary layer characteristics using a 1-D PBL model over the Bay of Bengal during BOBMEX-99. *Proceedings of Indian Academy of Sciences (Earth and Planetary Sciences)*, **112**, 185–204.
- Satyanarayana, A. N. V., U. C. Mohanty, S. N. Devdutta, T. Sethuraman, V. N. Lykossov, H. Warrior, and N. V. Sam, 2001: A study on marine boundary layer processes in the ITCZ and non ITCZ regimes over Indian Ocean with INDOEX IFP-99 data. *Current Science*, **80**, 39–45.
- Shinoda, T., H. H. Hendon, and J. G. Glick, 1998: Intra seasonal sea surface temperature variability in the tropical pacific and Indian Ocean. *J. Climate*, **11**, 1685–1702.
- Shukla, J., D. Strauss, D. Randall, Y. Sud, and L. Marx, 1981: Winter and summer simulations with the GLAS climate model, NASA Technical Memo, 83866, 282pp.
- Sikka, D. R., and S. Gadgil, 1980: On the maximum cloud zone and the ITCZ over Indian longitudes during southwest monsoon. *Mon. Wea. Rev.*, **108**, 1840–1853.
- Smith, S. D., 1988: Coefficients for sea surface wind stress, heat flux and wind profiles as a function of wind speed and temperature. *J. Geophys. Res.*, **93**, 15467–15472.
- Stull, R. B., 1997: *An Introduction to Boundary Layer Meteorology*. Kluwer Academic Publishers, 664pp.
- Torrence, C., and G. P. Compo, 1998: A practical guide to wavelet analysis. *Bull. Amer. Meteor. Soc.*, **79**, 61–78.
- Webster, P. J., and R. Lukas, 1992: TOGA COARE: The coupled ocean atmosphere response experiment. *Bull. Amer. Meteor. Soc.*, **73**, 1377–1416.
- Wentz, F. J., 1986: Users manual SEASAT scatterometer wind vectors. RSS technical report, 081586, Remote sensing systems, Santa Rosa, CA, 21pp.
- Wyrtki, K., 1973: An equatorial jet in the Indian Ocean. *Science*, **181**, 262–264.
- Yasunari, T., 1979: Cloudiness fluctuations associated with the northern hemisphere summer monsoon. *J. Meteor. Soc. Japan*, **57**, 227–242.
- Yasunari, T., 1981: Structure of an Indian summer monsoon system with around 40-day period. *J. Meteor. Soc. Japan*, **59**, 336–354.